

Gluons in two-color QCD at high baryon density

V. G. Bornyakov^{a,b,c} and R. N. Rogalyov^a

a) Institute for High Energy Physics NRC "Kurchatov Institute", 142281 Protvino, Russia

b) School of Biomedicine, Far East Federal University, 690950 Vladivostok, Russia

*c) Institute of Theoretical and Experimental Physics NRC "Kurchatov Institute",
117259 Moscow, Russia*

January 7, 2021

Abstract

Landau gauge longitudinal and transverse gluon propagators are studied in lattice QCD with gauge group $SU(2)$ at varying temperature and quark density. In particular, it is found that the longitudinal propagator decreases with increasing quark chemical potential at all temperatures under study, whereas the transverse propagator increases with increasing quark chemical potential at $T < 200$ MeV and does not depend on it at higher temperatures. The relative strength of chromoelectric and chromomagnetic interactions is also discussed.

1 Introduction

We study Landau gauge gluon propagators in $N_f = 2$ lattice QCD with gauge group $SU(2)$ at nonzero temperature and quark density. The details of the lattice action used to generate the gauge field configurations are described in recent papers[1, 2].

It is well known that lattice QCD approach is very successful at zero baryon density but is inapplicable so far at high baryon density due to the so called sign problem [3]. It is then useful to study in the lattice regularization the theories similar to QCD (QCD-like) but without sign problem. In particular, QCD with $SU(2)$ gauge group [4] (to be called below QC_2D) is one of such theories.

QC₂D was studied using various approaches which are also applicable to QCD at high baryon density. It is thus possible to check their predictions in the case of QC₂D confronting respective results with first principles lattice results.

The phase diagram of QC₂D in the $T - \mu_q$ plane is still not fixed solidly. In the studies of the $N_f = 2$ lattice QC₂D with staggered fermionic action at high quark density and $T = 0$ it was demonstrated[1] that the string tension σ decreases with increasing μ_q and becomes compatible with zero for μ_q above 850 MeV. In a more recent paper [5], where $N_f = 2$ lattice QC₂D with Wilson fermionic action was studied, the authors did not find the confinement-deconfinement transition at low temperature. The reason for this discrepancy might be the lattice artifacts at large lattice values of $\mu_q a$.

In this paper we make a step toward the study of QC₂D phase diagram in the $T - \mu_q$ plane. We concentrate on the study of the Landau gauge gluon propagators at nonzero temperature and varying quark chemical potential and compare the results with our earlier findings obtained at zero temperature. We try to find the signs of the confinement-deconfinement transition in the gluon propagators dependence on the temperature and the quark chemical potential.

The gluon propagators are among important quantities to study, e.g. they play crucial role in the Dyson-Schwinger equations approach. The μ_q and/or temperature dependence of the gluon propagators in Landau gauge in lattice QC₂D were studied before in Refs. [6, 7, 8, 9].

One of the conclusions of Ref. [9] was that, beyond the hadronic phase in the $\mu_q - T$ phase diagram of QC₂D, the chromoelectric interactions are suppressed at low momenta, whereas the chromomagnetic - practically do not change.

The gluon propagators in QC₂D at nonzero μ_q were also studied in Ref. [10] with help of the Dyson-Schwinger equations approach and in Ref. [11] using the massive Yang-Mills theory approach at one-loop. The authors emphasize that after the agreement with the lattice results for the gluon propagators will be reached their methods could be applied to real QCD at nonzero baryon density. Thus to provide unbiased lattice results is very important.

Our computations are completed on lattices 32^4 , $32^3 \cdot 24$, $32^3 \cdot 16$, $32^3 \cdot 8$ with respective temperature values¹ $T = 0, 188, 280, 560$ MeV and quark chemical potential $0 \leq \mu_q < 1.8$ GeV. The lattice spacing for parameters used in this study was determined in Ref.[1] as $a = 0.044$ fm. In this work

¹Strictly speaking, for our symmetric 32^4 lattice, $\frac{1}{N_t a} = 140$ MeV. We consider this value as a good approximation for zero temperature in accordance with common practice.

we do not determine the line of confinement-deconfinement transition in $T - \mu_q$ plane leaving this important task to future studies. It is pretty clear that $T = 560$ MeV is in the deconfinement phase for any value of μ_q . Same is true for $T = 280$ MeV, most probably. We expect that $T = 188$ MeV is in the confinement phase at $\mu_q = 0$ and transition to the deconfinement phase happens at high μ_q .

2 Gluon propagators

The analysis of our data indicates that both the longitudinal and the transverse propagators are decreasing functions of the momentum; our data can be described using the fit function

$$D_{L,T}(p) = Z_{L,T} \frac{1 + \delta_{L,T} p^2}{p^4 + 2R_{L,T} p^2 + M_{L,T}^2}, \quad (1)$$

which, in particular, stems from the Refined Gribov-Zwanziger approach [12]. It has received considerable attention in the literature [13, 14, 16, 17, 15]. The respective fitting procedure was considered in detail in Refs. [18, 19] at $T = 0$, here we describe the results for higher temperatures. We use the usual normalization condition for the propagators,

$$D_{L,T}^{ren}(\kappa^2) = \frac{1}{\kappa^2}, \quad (2)$$

at $\kappa = 6$ GeV. Below we consider renormalized quantities omitting superscript 'ren'. We consider only the soft modes $p_4 = 0$.

2.1 Dressing functions

The gluon dressing functions

$$J_{L,T}(p) = p^2 D_{L,T}(p) \quad (3)$$

as well as the curves derived from the Gribov-Stingl fit (1) are shown in Fig.1. It should be emphasized that the zero-momentum propagator values were taken into account in the fit; the respective information is encoded in the behavior of the dressing functions at $p \rightarrow 0$.

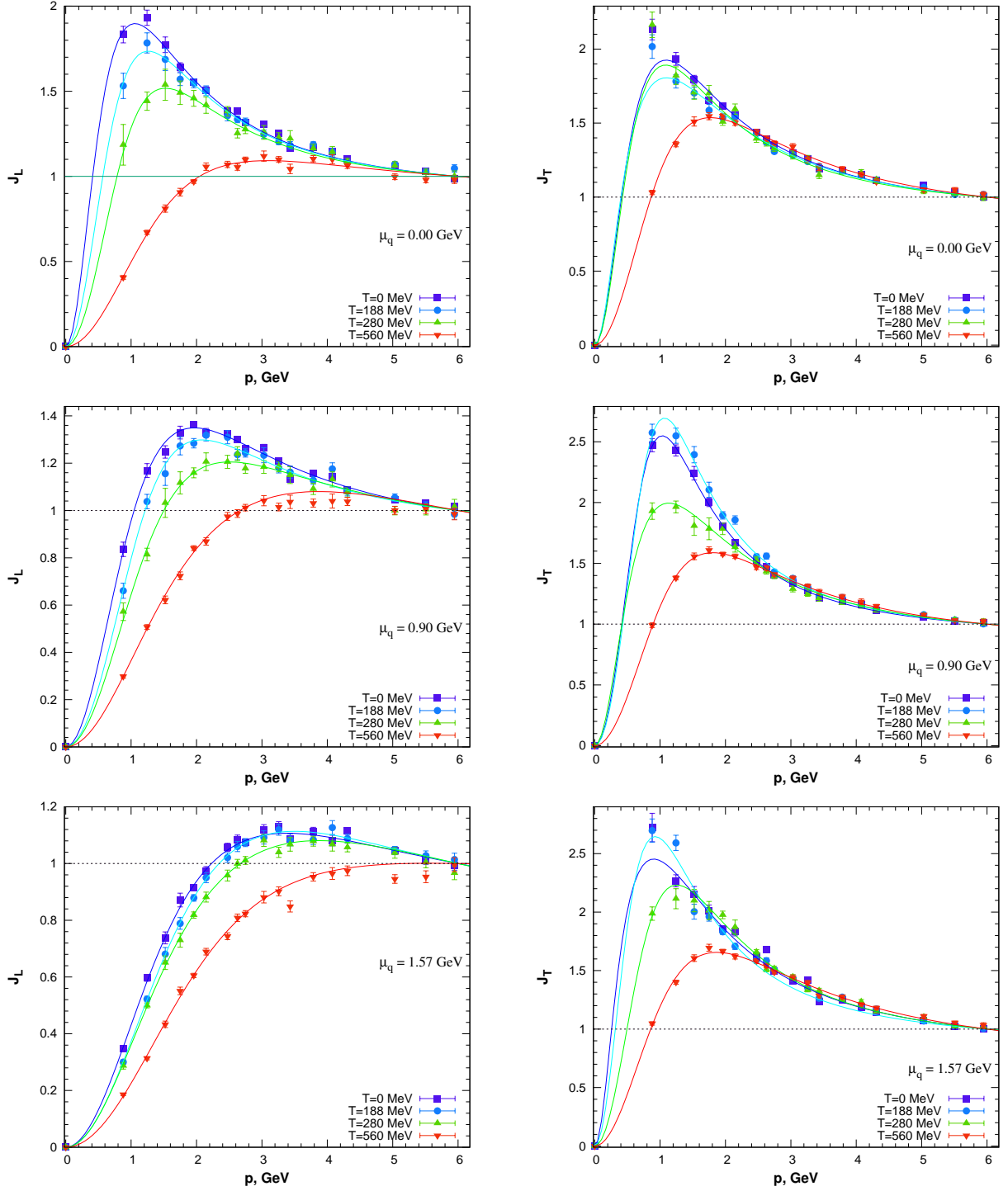


Figure 1: Longitudinal (left column) and transverse (right column) gluon dressing functions at $\mu_q = 0.00$ (first row), $\mu_q = 0.90$ GeV (second row), and $\mu_q = 1.57$ GeV (third row) for four temperatures.

In general, a shape of the dressing functions is similar to that in pure gluodynamics at finite temperature; specific features of their behavior are as follows.

When we increase either T or μ_q (or both) the value of the momentum at which the **longitudinal** dressing function J_L has a maximum increases, the width of the peak also increases, while the maximal value of the dressing function decreases. At high T and/or μ_q , J_L tends to that of a free massive particle; at $T = 560$ MeV and $\mu_q = 1.57$ GeV it comes close to the dressing function of a free particle of mass $m \approx 2$ GeV.

A completely different situation is observed in the **transverse** case. At $T = 560$ MeV the dressing function is practically independent of μ_q ; at lower temperatures the peak position does not depend on μ_q , whereas the peak value moderately increases with increasing μ_q , the width of the peak depends only weakly on μ_q . Therewith, an increase of the temperature at a given chemical potential gives (i) an increase of the peak position, (ii) a decrease of the peak value, (iii) a moderate increase of the peak width. The transverse gluon dressing functions at all temperatures under study coincide at momenta above ≈ 2 GeV for $\mu_q = 0$ and at momenta above ≈ 2.5 GeV for high μ_q values. This is an indication of smallness of the magnetic screening mass at all values of T and μ_q .

2.2 Temperature dependence at various momenta and quark chemical potentials

Both propagators change only a little when the temperature varies below 280 MeV, whereas they show a significant decrease as the temperature increases from $T = 280$ MeV to $T = 560$ MeV.

This being so, temperature dependence of **the longitudinal propagator** is substantial at $p \lesssim 4$ GeV at small μ_q and it is seen up to the normalization point $p = 6$ GeV at high μ_q . In the infrared, the longitudinal propagator decreases significantly with the temperature at $\mu_q \lesssim 1.2$ GeV, whereas at greater values of μ_q it shows a less pronounced decrease. This can be seen also in Fig. 2 (left, upper row) where dependence of the propagators at zero momentum on temperature and quark chemical potential are depicted. The value of $D_{L,T}(0)$ is of special importance since it is used in one of the definitions of the screening mass, see, e.g. review Ref. [20].

Temperature dependence of **the transverse propagator** is seen only at relatively low momenta ($p \lesssim 2 \div 2.5$ GeV) as was already said above. Similar to the longitudinal case, it decreases with temperature. However, in contrast to the longitudinal propagator, its variation with the temperature

increases with increasing μ_q (see also Fig.2 (right)).

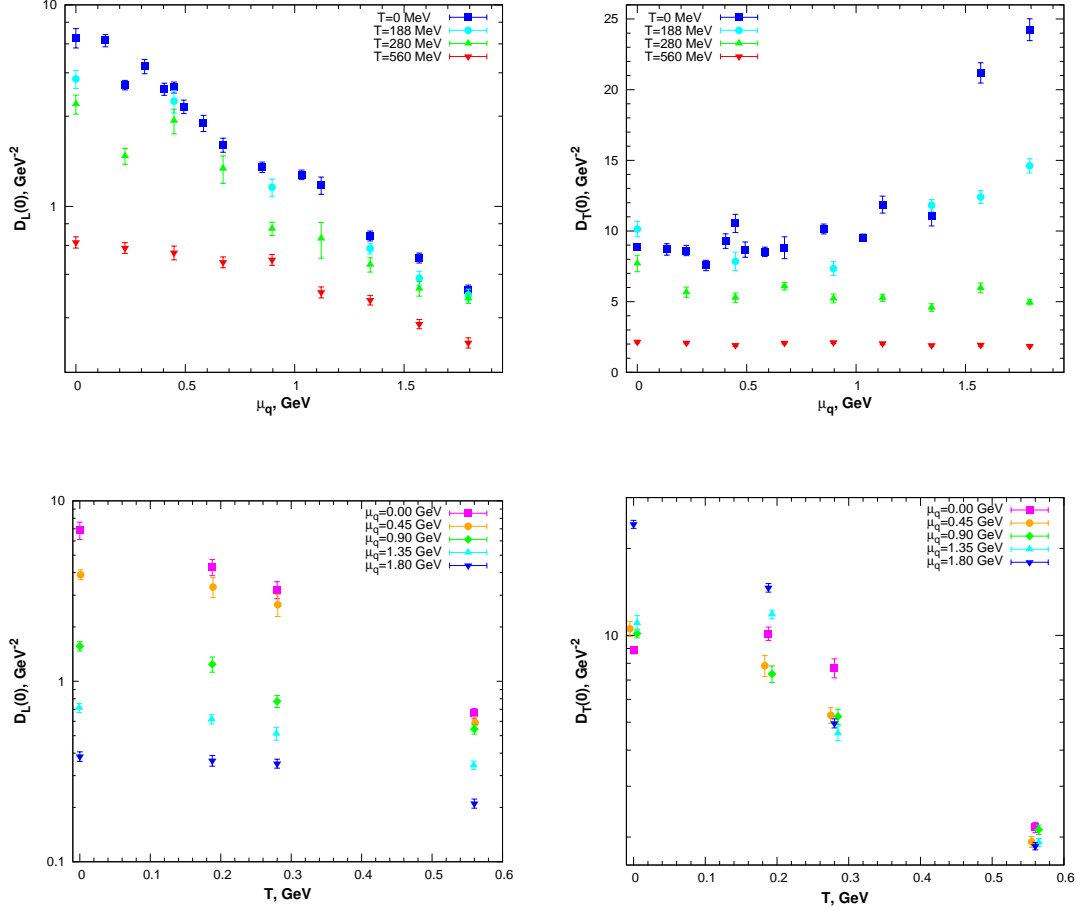


Figure 2: Zero-momentum longitudinal (left column) and transverse (right column) gluon propagators as functions of μ_q at various temperatures (upper row) and as functions of T at various μ_q (lower row).

2.3 The dependence on the quark chemical potential at various momenta and temperatures

The longitudinal propagator gradually decreases with the chemical potential at all momenta ($p \leq 6$ GeV) and temperatures under consideration. The decreasing is more pronounced at low momenta and temperatures.

The transverse propagator at low momenta and temperatures ($T < 200$ MeV, $p \lesssim 2 \div 2.5$ GeV) and $\mu_q \gtrsim 1$ GeV increases with increasing μ_q . At $T = 280$ MeV its dependence on μ_q becomes less pronounced and it disappears completely at $T = 560$ MeV. At high momenta the transverse propagator is independent of μ_q at all temperatures.

3 Screening masses and interaction potentials

3.1 Definition of the screening mass

In the general case, a widely used definition of the screening mass stems from the on-mass-shell renormalization of the propagator: the inverse propagator is considered as a regular function in some neighborhood of $p^2 = 0$ and thus represented in the form

$$D_{L,T}^{-1}(p) = Z^{-1}(m_{E,M}^2 + \tilde{\Pi}(p^2) + p^2), \quad (4)$$

where the Taylor expansion of the function $\tilde{\Pi}(p^2)$ starts from the order $O((p^2)^2)$ terms. The propagator of renormalized fields $A_R = Z^{-1/2}A$ has the form

$$D_{L,T}^{ren}(p) = \frac{1}{m_{E,M}^2 + p^2 + \tilde{\Pi}(p^2)} \quad (5)$$

and, if $\tilde{\Pi}(p^2)$ is small in the infrared, it has a pole at $p^2 \approx -m_{E,M}^2$. Thus the parameter $m_{E,M}$ can be associated both with the mass of the particle and with the asymptotic behavior of the propagator at spatial infinity

$$D_{L,T}(0, \vec{x}) \simeq C_{E,M} e^{-m_{E,M}|\vec{x}|}. \quad (6)$$

In Refs. [21, 22, 23] the chromoelectric and chromomagnetic screening masses were determined using the Yukawa-type fit function

$$D_{L,T}^{-1}(p) = Z_{E,M}^{-1}(m_{E,M}^2 + p^2) \quad (7)$$

at zero and finite temperatures. It was shown [23] that the Yukawa-type fit function (7) provides a good quality of this fit over rather wide range of momenta giving evidence for smallness of $\tilde{\Pi}(p^2)$ in the infrared.

The above definition of $m_{E,M}^2$ can be related to the correlation length:

$$m_{E,M}^2 = \xi_{E,M}^{-2}, \quad (8)$$

where the correlation length $\xi_{E,M}$ is conventionally defined in terms of the correlation function (propagator in our case) by the expression [24]

$$\xi^2 = \frac{1}{2} \frac{\int_V dx_4 d\vec{x} \tilde{D}(x_4, \vec{x}) |\vec{x}|^2}{\int_V dx_4 d\vec{x} D(x_4, \vec{x})} = -\frac{1}{2D(0, \vec{0})} \sum_{i=1}^3 \left(\frac{d}{dp_i} \right)^2 \Big|_{\vec{p}=0} D(0, \vec{p}) . \quad (9)$$

We consider definition of the screening masses based on the fit of $D_{L,T}^{-1}(p)$ at low momenta to a polynomial in p^2 :

$$D_{L,T}^{-1}(p) = Z_{E,M}^{-1} (m_{E,M}^2 + p^2 + c_4 \cdot (p^2)^2 + \dots) . \quad (10)$$

This method was used in Refs. [25, 18]. However, we use the function (10) rather than function (7) because we have not enough data points in the infrared region where the propagator can be described by the function (7). Thus, to obtain reasonable fit results we had to use terms up to $(p^2)^2$ for $D_L(p)$ and terms up to $(p^2)^3$ for $D_T(p)$. Still, we hope that making use of the fit function (10) provides reasonably good estimates of the parameters in eq. (7).

When the screening masses are large, it is natural to assume that the one-gluon exchange dominates. In the approximation of one-gluon exchange, the potential of chromoelectrostatic interaction between static external color sources is given by the Fourier transform of the longitudinal propagator (the chromomagnetostatic potential between currents - by the Fourier transform of the transverse propagator). Both chromoelectric and chromomagnetic potentials are short-range; that is, they can be roughly described by a potential well of certain width and depth. The parameter characterizing the width is provided by $\xi_{E,M} = \frac{1}{m_{E,M}}$, whereas the parameter $V_{E,M}$ characterizing the depth can be defined as follows:

$$\int d\vec{x} \mathcal{V}_{E,M}(\vec{x}) = D_{L,T}(p_4 = 0, \vec{p} = 0) = V_{E,M} \xi_{E,M}^3 \quad (11)$$

$$\implies V_{E,M} = D_{L,T}(0) m_{E,M}^3 , \quad (12)$$

where $\mathcal{V}_{E,M}(\vec{x})$ is the chromoelectric (chromomagnetic) potential describing interaction between static color charges (currents).

Before proceeding further, we recollect again another definition of the screening mass [20]:

$$\mathcal{M}_E^2 = \frac{1}{D_L(0)} , \quad \mathcal{M}_M^2 = \frac{1}{D_T(0)} . \quad (13)$$

Clearly, it depends on renormalization and is rather sensitive to the finite volume effects. Loosely speaking, eq. (13) characterizes “the total amount” of the interaction since

$$\frac{1}{\mathcal{M}_{E,M}^2} = \int dx_4 d\vec{x} D_{L,T}(x_4, \vec{x}) = \int d\vec{x} \mathcal{V}_{E,M}(\vec{x}), \quad (14)$$

where $D_{L,T}(x_4, \vec{x})$ are the propagators in the coordinate representation.

It follows from (12) and (10) that

$$V_{E,M} = Z_{E,M} m_{E,M}, \quad (15)$$

where $Z_{E,M}$ is the respective renormalization factor. The numerical results for $V_{E,M}$ will be presented below.

3.2 Dependence of screening masses and interaction potentials on μ_q and T

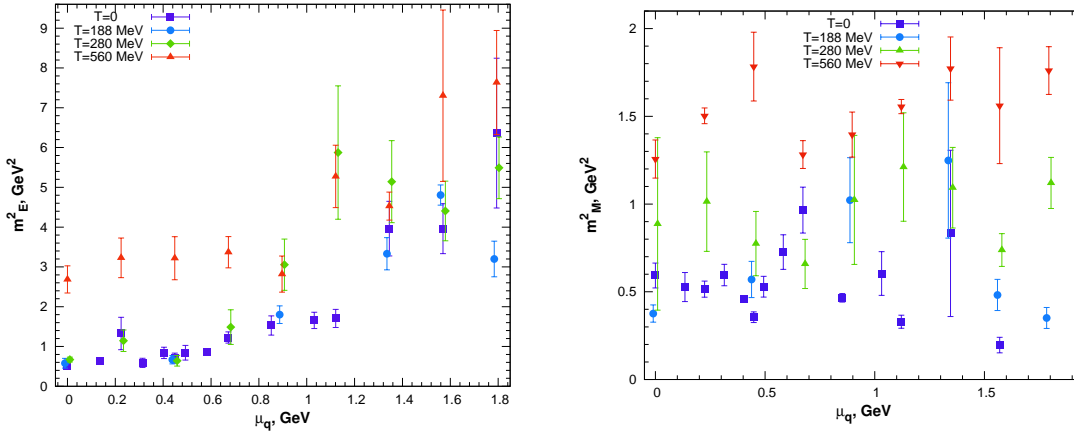


Figure 3: Chromoelectric (left) and chromomagnetic (right) screening masses as functions of μ_q at various temperatures.

In Fig.3 we show the electric (left panel) and magnetic (right panel) masses as functions of the quark chemical potential at various temperatures.

Our value for $m_E/\sqrt{\sigma}$ at $\mu_q = 0$ and $T = 0$ is 1.50(4) [18]. This value should be compared with the value 1.47(2) obtained in SU(3) gluodynamics

at zero temperature [22] by fitting the inverse propagator to the form (7) at small momenta². We also quote a value 1.48(5) obtained for a mass dominating the small momentum behavior of a gluon propagator in $SU(2)$ lattice gluodynamics in [26].

At temperatures $T \leq 300$ MeV, m_E does not significantly change at small μ_q corresponding to the hadron phase. Above $\mu_q \approx 200$ MeV it starts to increase and continues to increase up to 1.8 GeV. This behavior is analogous to that of the electric screening mass in QCD at $T > T_c$ as was demonstrated by lattice simulations [27, 28, 23, 21]. No such increasing was reported in the earlier studies[9] of QC₂D.

	$\mu_q < 850$ MeV	$\mu_q > 850$ MeV
$T < 300$ MeV	$m_E \simeq 0.7$ GeV $m_M \simeq 0.7$ GeV	$m_E \simeq 1.8 \div 2.4$ GeV $m_M \simeq 0.4 \div 1.1$ GeV
$T = 560$ MeV	$m_E \simeq 1.6 \div 1.8$ GeV $m_M \simeq 1.2 \div 1.3$ GeV	$m_E \simeq 2.4 \div 3.0$ GeV $m_M \simeq 1.3 \div 1.5$ GeV

Table 1: Dependence of the screening masses on the quark chemical potential and temperature. It should be emphasized that, at $T = 0$ and $\mu_q > 850$ MeV, the magnetic mass decreases from $m_M \simeq 700$ MeV to $m_M \simeq 400$ MeV.

Information on the behavior of the screening masses is summarized in the table. Chromoelectric forces feature the longest range at $T = 0$ and $\mu_q = 0$; their screening increases with an increase of both T and μ_q .

Chromomagnetic forces have the same radius as chromoelectric at $T = 0$ and $\mu_q = 0$; however, their screening increases with T , whereas μ_q -dependence of their screening depends on the temperature: m_M decreases with μ_q at low temperatures, remains constant at $T = 280$ MeV and tends to increase at $T = 560$ MeV.

It should be emphasized that an increase of m_M is clearly seen provided that high temperatures are taken into consideration. No such increase was observed in Ref. [9] where the temperature range $T < 1.6T_c$ was investigated; in this temperature range our data tend to confirm the previous results: a very limited growth of m_M is observed at $T < 280$ MeV.

²We obtained this value taking mass value 647(7) MeV, obtained in [22] and dividing it by $\sqrt{\sigma} = 440$ MeV used in [22] to set the scale.

It should also be noticed that the Z factors obtained here differ from the ratio

$$\eta_{E,M}(\mu_q) = \frac{m_{E,M}^2(\mu_q)}{\mathcal{M}_{E,M}^2(\mu_q)} = m_{E,M}^2(\mu_q) D_{L,T}(0) \quad (16)$$

considered in our previous study [18]. The reason is as follows: we obtain Z from the fitting procedure, which is in fact equivalent to making use of the formula (16), however, with $D_{L,T}(0)$ evaluated as zero-momentum value of the fit function (10) rather than the value extracted from data immediately.

In our previous study [18] devoted to zero-temperature case, Z_E was considered as independent of μ_q apart from variation at small μ_q values. However, in the present study we found that both Z_E and Z_M depend either on μ_q or on T .

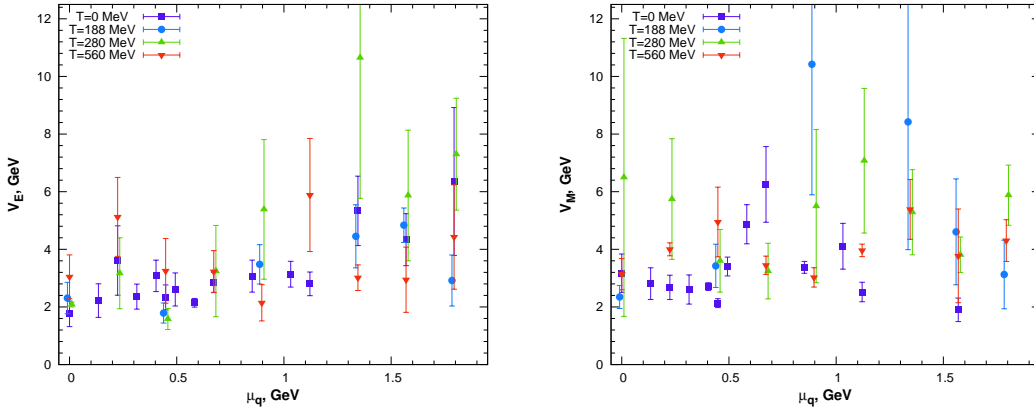


Figure 4: The parameter $V_{E,M}$ characterizing interaction between color static sources as functions of the quark chemical potential at various temperatures. Huge errors make only qualitative estimates possible.

The depth of the potential well can be roughly estimated from the formula (15), the results are shown in Fig.4. It varies over the range $2 \lesssim V_{E,M} \lesssim 6$ GeV. Huge errors do not allow to perform quantitative comparison of V_E with V_M , as seen by eye, V_M tends to be a little greater.

4 Conclusions

- We investigated the dependence of D_T and D_L on the temperature and isospin chemical potential. Both propagators decrease with increas-

ing temperature; however, they behave differently as the functions of μ_q . D_L decreases with increasing μ_q at all temperatures under study, whereas D_T increases with increasing μ_q at $T < 200$ MeV and is independent of μ_q at higher temperatures.

- In the model under study, the radius of action of the chromomagnetic forces is greater than that of chromoelectric forces at all temperatures and chemical potentials excepting a neighborhood of the point $\mu_q = 0, T = 0$. Within the range of action, the strength of chromomagnetic forces is also approximately the same or a little greater than that of chromoelectric ones (at $\mu_q > 0, T > 0$). For this reason, the strong interacting matter described by QC_2D at nonzero temperatures and quark chemical potentials can be named a chromomagnetic medium.

Acknowledgments

The work was completed due to support of the Russian Foundation for Basic Research via grant 18-02-40130 mega. The authors are thankful to Victor Braguta, Andrey Kotov and Alexander Nikolaev for providing gauge field configurations and useful discussions. The research is carried out using the Central Linux Cluster of the NRC “Kurchatov Institute” - IHEP, the equipment of the shared research facilities of HPC computing resources at Lomonosov Moscow State University, the Linux Cluster of the NRC “Kurchatov Institute” - ITEP (Moscow). In addition, we used computer resources of the federal collective usage center Complex for Simulation and Data Processing for Mega-science Facilities at NRC Kurchatov Institute, <http://ckp.nrcki.ru/>.

References

- [1] V. Bornyakov, V. Braguta, E. M. Ilgenfritz, A. Y. Kotov, A. Molochkov and A. Nikolaev, JHEP **03**, 161 (2018) [arXiv:1711.01869 [hep-lat]].
- [2] N. Astrakhantsev, V. Bornyakov, V. Braguta, E. M. Ilgenfritz, A. Kotov, A. Nikolaev and A. Rothkopf, JHEP **05**, 171 (2019) [arXiv:1808.06466 [hep-lat]].
- [3] S. Muroya, A. Nakamura, C. Nonaka and T. Takaishi, Prog. Theor. Phys. **110**, 615-668 (2003) [arXiv:hep-lat/0306031 [hep-lat]].

- [4] J. Kogut, M. A. Stephanov, D. Toublan, J. Verbaarschot and A. Zhitnitsky, Nucl. Phys. B **582**, 477-513 (2000) [arXiv:hep-ph/0001171 [hep-ph]].
- [5] T. Boz, P. Giudice, S. Hands and J. I. Skullerud, Phys. Rev. D **101**, no.7, 074506 (2020) [arXiv:1912.10975 [hep-lat]].
- [6] S. Hands, S. Kim and J. I. Skullerud, Eur. Phys. J. C **48**, 193 (2006) [arXiv:hep-lat/0604004 [hep-lat]].
- [7] T. Boz, S. Cotter, L. Fister, D. Mehta and J. I. Skullerud, Eur. Phys. J. A **49**, 87 (2013) [arXiv:1303.3223 [hep-lat]].
- [8] O. Hajizadeh, T. Boz, A. Maas and J. I. Skullerud, EPJ Web Conf. **175**, 07012 (2018) [arXiv:1710.06013 [hep-lat]].
- [9] T. Boz, O. Hajizadeh, A. Maas and J. I. Skullerud, Phys. Rev. D **99**, no.7, 074514 (2019) [arXiv:1812.08517 [hep-lat]].
- [10] R. Contant and M. Q. Huber, Phys. Rev. D **101**, no.1, 014016 (2020) doi:10.1103/PhysRevD.101.014016 [arXiv:1909.12796 [hep-ph]].
- [11] D. Suenaga and T. Kojo, Phys. Rev. D **100**, no.7, 076017 (2019) doi:10.1103/PhysRevD.100.076017 [arXiv:1905.08751 [hep-ph]].
- [12] D. Dudal, J. A. Gracey, S. P. Sorella, N. Vandersickel and H. Verschelde, Phys. Rev. D **78**, 065047 (2008) [arXiv:0806.4348 [hep-th]].
- [13] D. Dudal, O. Oliveira and N. Vandersickel, Phys. Rev. D **81**, 074505 (2010) [arXiv:1002.2374 [hep-lat]].
- [14] A. Cucchieri, D. Dudal, T. Mendes and N. Vandersickel, Phys. Rev. D **85**, 094513 (2012) [arXiv:1111.2327 [hep-lat]].
- [15] R. Aouane, V. Bornyakov, E. Ilgenfritz, V. Mitrjushkin, M. Muller-Preussker and A. Sternbeck, Phys. Rev. D **85**, 034501 (2012) [arXiv:1108.1735 [hep-lat]].
- [16] O. Oliveira and P. J. Silva, Phys. Rev. D **86**, 114513 (2012) [arXiv:1207.3029 [hep-lat]].
- [17] D. Dudal, O. Oliveira and P. J. Silva, Annals Phys. **397**, 351-364 (2018) [arXiv:1803.02281 [hep-lat]].
- [18] V. Bornyakov, A. Kotov, A. Nikolaev and R. Rogalyov, Particles **3**, no.2, 308-319 (2020) [arXiv:1912.08529 [hep-lat]].
- [19] V. Bornyakov, V. Braguta, A. Nikolaev and R. Rogalyov, [arXiv:2003.00232 [hep-lat]].

- [20] A. Maas, Phys. Rept. **524** (2013), 203-300 [arXiv:1106.3942 [hep-ph]].
- [21] V. Bornyakov and V. Mitrjushkin, Phys. Rev. D **84**, 094503 (2011) [arXiv:1011.4790 [hep-lat]].
- [22] O. Oliveira and P. Bicudo, J. Phys. G **38**, 045003 (2011) [arXiv:1002.4151 [hep-lat]].
- [23] P. Silva, O. Oliveira, P. Bicudo and N. Cardoso, Phys. Rev. D **89**, no.7, 074503 (2014) [arXiv:1310.5629 [hep-lat]].
- [24] S. Ma, Modern Theory of critical phenomena (W. A. Benjamin, Advanced Book Program, Minnesota University, 1976).
- [25] V. Bornyakov and V. Mitrjushkin, Int. J. Mod. Phys. A **27**, 1250050 (2012) [arXiv:1103.0442 [hep-lat]].
- [26] K. Langfeld, H. Reinhardt and J. Gattnar, Nucl. Phys. B **621**, 131-156 (2002) [arXiv:hep-ph/0107141 [hep-ph]].
- [27] C. S. Fischer, A. Maas and J. A. Muller, Eur. Phys. J. C **68**, 165-181 (2010) [arXiv:1003.1960 [hep-ph]].
- [28] A. Maas, J. M. Pawłowski, L. von Smekal and D. Spielmann, Phys. Rev. D **85**, 034037 (2012) [arXiv:1110.6340 [hep-lat]].